Third International Conference on CFD in the Minerals and Process Industries
CSIRO, Melbourne, Australia
10-12 December 2003

COMPARISON OF TURBULENT SCALAR TRANSPORT IN A PIPE AND A ROTATING CYLINDER

Matthew BILSON[1] and Klaus BREMHORST[1]

[1] Division of Mechanical Engineering, The University of Queensland, Brisbane, Queensland 4072, AUSTRALIA

ABSTRACT

The rotating cylinder (RC) is frequently used for investigation of flow accelerated corrosion (FAC), as it allows for good control over electrochemical conditions. To make RC measurements useful a method of transferring results to a different configuration is required. It has been hypothesized that by matching wall shear stress in two configurations, similar transport mechanisms and hence similar corrosion rates will result.

Direct numerical simulation was used to compare mass transport, which was considered in the context of a passive scalar, for turbulent flow in a RC to a straight pipe (SP). For the SP the Reynolds number was set to 2650, and for the RC the Reynolds number was 3200. The Reynolds numbers were chosen to give approximately equal wall shear stress. For the scalar transport both simulations used Sc=0.71 and Sc=5.0.

For the SP it was found that scalar transport was due to turbulent convection and molecular diffusion. Turbulent flow in the RC contains turbulent Taylor vortices. It was found that these vortices made up a significant fraction of the total scalar transport, meaning that the scalar transport mechanisms in the two configurations were different.

NOMENCLATURE

c scalar concentration
k mass transfer coefficient
L cylinder length
p pressure
q scalar flux
R pipe radius
R_1 inner cylinder radius
R_2 outer cylinder radius
Re Reynolds number,
pipe: $Re = U_b R/\nu$
rotating cylinder: $Re = U_1(R_2-R_1)/\nu$
Re_τ friction velocity Reynolds number
Sc Schmidt number (ν/α)
Sh Sherwood number ($2kR/\alpha$)
t time
U_b bulk velocity (pipe)
U_1 tangential velocity of inner cylinder
u velocity vector
u velocity in x for pipe, in z for rotating cylinder
u_τ friction velocity $(\tau_w/\rho)^{1/2}$
v velocity in y for pipe and rotating cylinder
w velocity in z for pipe, in x for rotating cylinder
x axial coordinate
y radial coordinate
z azimuthal coordinate
$\langle\rangle$ averaged quantity, averaging is in xzt unless otherwise stated
$\langle\rangle_x$ quantity averaged in x

Greek Letters

α diffusivity
Δ grid spacing
η radius ratio (R_1/R_2)
Γ aspect ratio ($L/(R_2-R_1)$)
λ Taylor vortex pair wavelength
ν kinematic viscosity
ρ density
τ_w mean wall shear stress in direction of mean flow

Subscripts

1 inner cylinder quantity
2 outer cylinder quantity
i coordinate direction
rms root mean square value of a fluctuating quantity

Superscripts

+ wall unit
′ fluctuation (due to turbulence in the pipe, turbulence and TV in the rotating cylinder)
″ fluctuation due to turbulence in the rotating cylinder

INTRODUCTION

In flow accelerated corrosion (FAC), fluid flow causes an increase in the rate of transport of chemical species to/from the metal surface, resulting in an increase of the corrosion rate. FAC is classified as mass transport controlled when diffusion of reacting species limits the corrosion rate. The design and construction of laboratory based facilities for studying FAC is a difficult task, as good control over the electrochemistry is required. A more economical apparatus is the rotating cylinder (RC) (Gabe et al., 1998). It consists of a RC immersed in a container of fluid. The immersed cylinder is rotated to incorporate the effects of fluid flow on the corrosion process. The apparatus allows for full control over thermal, electrochemical and hydrodynamic conditions. The major disadvantage of the RC is that no universal configuration exists and hence relations for mass transport vary significantly (Poulson, 1983).

To make RC measurements useful a method of transferring results from the RC to a different configuration is required. In this paper the alternate configuration will be taken to be a straight pipe (SP), since it is a practical configuration where corrosion can have drastic consequences. Methods to transfer RC results rely on the assumption that electrochemical conditions are matched, and the problem is then reduced to one of determining what hydrodynamic conditions will cause

Copyright © 2003 CSIRO Australia

mass transfer rates to be similar. Parameters such as velocity, wall shear stress, turbulence intensity and Sherwood number have been proposed (Poulson, 1993).

Wall shear stress is a parameter that has received significant attention for transfer of RC results. It has been hypothesized that for approximately equal wall shear stress in two configurations, the result will be similar transport mechanisms and overall mass transfer rates (Silverman, 1984). For very high Schmidt numbers (Sc~1000) the diffusion layer lies well within the laminar sub-layer. The velocity profile is linear and proportionality between wall shear stress and mass transfer can be proven (Levich, 1962). However, care must be taken when using wall shear stress to transfer results because zero wall shear stress does not automatically give zero mass transfer. For example, flow over a cylinder will have zero shear stress at the separation points, but mass transfer could still occur (Levich, 1962). Hence, wall shear stress must only be used to transfer results between similar flows.

Although proportionality between shear stress and mass transfer exists at a large Schmidt number, there is no evidence that equal wall shear stress in two different configurations will result in any similarity between mass transport mechanisms. Therefore, the aim of this paper is to compare mass transport mechanisms, for turbulent flow in a SP to turbulent flow in a RC, under the condition of approximately equal wall shear stress.

To complete the objective direct numerical simulation (DNS) will be used. DNS is the most computationally expensive method of flow simulation, as it resolves down to the smallest scales of turbulent motion. The advantage of DNS is that no turbulence model is required and the results are an exact representation of turbulence. Computer resources limit DNS to simple configurations and low Reynolds and Schmidt numbers (e.g. for pipe flow Re≈5000 and Sc≈5). In corrosion processes the Schmidt number is typically around 1000. Although DNS can not achieve this, the present work can still contribute by examining the trends that occur for increasing Schmidt number (e.g. Sc=0.71 versus Sc=5.0).

PREVIOUS WORK

Straight Pipe

The structure and statistics of turbulent pipe flow and mass transfer have been thoroughly investigated. Pope (2000) gives the most recent account of turbulent pipe flow and Kawamura et al. (1998) report DNS of heat transfer in channel flow up to Sc=5. The turbulence statistics for pipe flow are virtually identical to channel flow (Pope, 2000).

Rotating Cylinder

Configuration

Several different configurations of the RC have used for corrosion experiments (Gabe et al., 1998). In almost every case the flow is turbulent. For the purpose of this paper a simplified RC configuration is adopted. It consists of two concentric cylinders of theoretically infinite length, with the inner cylinder rotating (figure 1). The Reynolds number, radius ratio (η) and aspect ratio (Γ) define the flow in the apparatus.

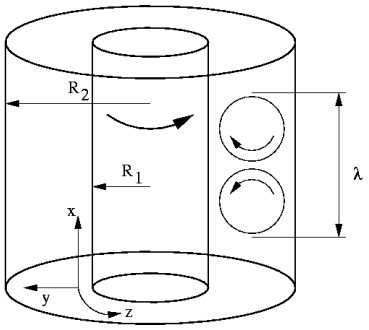

Figure 1: Ideal rotating cylinder configuration and Taylor vortex motion

Fluid Flow

The transition to turbulence and turbulent flow in the RC is remarkably different to turbulent flow in the SP. A series of laminar flow states exists for increasing Reynolds numbers: laminar Couette flow, Taylor vortex (TV) flow, wavy TV flow, modulated wavy TV flow, and turbulent TV flow (Andereck et al., 1986, Coles, 1965). The TV flow consists of pairs of counter rotating vortices imposed onto the mean flow caused by the cylinder rotation (figure 1). Turbulent flow in the RC is different to the SP because of the presence of the TV motion. This motion persists for Reynolds numbers several orders of magnitude beyond the onset of turbulence (Smith and Townsend, 1982).

Measurements of the mean and fluctuating velocity components were reported by Smith and Townsend (1982) for an apparatus with η=0.66. They made measurements with a hot-wire probe at a single axial location and were able to isolate the influence of the TV flow by applying a very small axial velocity and phase averaging. Their mean velocity measurements showed that a linear velocity profile (normalized by wall shear stress) existed near each cylinder wall. The fluctuating velocity was separated into turbulent and TV flow components. It was found that the contribution of the TV motion to velocity fluctuations was significant but decreased with increasing Reynolds number.

The majority of previous numerical work for the RC has employed DNS to study laminar flow states (Liao et al., 1999) or applied time averaged turbulence models to study the turbulent flow state (Kobayashi et al., 1999). Yuu and Umekage (1995) reported the only known DNS of turbulent flow in the RC for a device with η=0.88, Γ=20 and Re=1500.

Mass Transfer

Most previous studies of mass transfer in the RC have been concerned with measurement of overall mass transfer rates, and not with the mechanisms of mass transport. The most widely recognized investigation in the RC was reported by Eisenberg et al. (1954). Measurements of mass transfer were made at several axial locations, however the influence of any TV motion was not reported.

Kataoka et al. (1977) gave an account of how the TV motions influence mass transfer. They reported mass transfer measurements at the outer cylinder for a device with η=0.617 at a variety of Reynolds numbers (laminar and turbulent flow states). The results showed a significant axial variation of surface mass transfer due to the presence of the TV flow, thus confirming that there

may be significant differences in mass transfer mechanisms between the SP and RC.

SIMULATION DETAILS

Several assumptions were made for this work: the corrosion was uniform and mass transport controlled, chemical reactions and migration due to charge were neglected, local changes in concentration were small and the fluid was assumed to be Newtonian and incompressible. The consequence of these assumptions is that the corrosion process can be considered in the context of mass transfer where the concentration behaves as a passive scalar. The governing equations are the Navier-Stokes and convection-diffusion equations, equations 1 to 3. For the SP, the equations were normalized by pipe radius, bulk velocity and wall mass flux. For the RC the characteristic dimensions were the gap width between the cylinders, velocity of the inner cylinder and concentration at the inner cylinder. In both cases time was normalized by the characteristic length and velocity, and pressure (kinematic, i.e. divided by density) by the square of the characteristic velocity.

$$\nabla \cdot (\mathbf{u}) = 0 \tag{1}$$

$$\frac{\partial \mathbf{u}}{\partial t} + \nabla \cdot (\mathbf{uu}) = -\nabla p + \frac{1}{\mathrm{Re}} \nabla \cdot (\nabla \mathbf{u}) \tag{2}$$

$$\frac{\partial c}{\partial t} + \nabla \cdot (\mathbf{u}c) = \frac{1}{Sc\,\mathrm{Re}} \nabla \cdot (\nabla c) \tag{3}$$

Numerical Method

The equations were discretized in space using a second order accurate finite volume method on a staggered grid. The grid was based on a cylindrical coordinate system since this is well suited to the SP and RC configurations. It was uniform in the axial and azimuthal directions and non-uniform in the radial direction, with a finer grid employed near walls. The equations were advanced in time with a semi-implicit scheme, using a second order Adams-Bashforth method for explicitly advanced terms, and the Crank-Nicholson method for implicitly advanced terms. All terms were advanced explicitly in time, except for those that had a detrimental effect on the maximum allowed time step for numerical stability. For the Navier-Stokes equations, pressure correction was accomplished with a fractional step method. The Poisson equation for pressure correction was solved using Fourier transforms to uncouple the periodic directions, and a tri-diagonal solver to invert the matrix (Akselvoll, 1995).

For the SP, azimuthal convection and diffusion terms were advanced implicitly near the pipe center, and radial diffusion terms advanced implicitly near the pipe wall (Akselvoll and Moin, 1996). In the RC the radial diffusion terms were advanced implicitly since the grid was refined near the cylinder walls.

Straight Pipe Simulation Details

The boundary conditions were periodic in the axial and azimuthal directions and no slip at the pipe wall. The singularity at the pipe center was overcome by linear interpolation (Akselvoll, 1995). The flow was driven by a pressure gradient, which was adjusted at each time step such that the bulk velocity remained constant. For the scalar, the boundary conditions were periodic in the axial and azimuthal directions, and a constant scalar flux at the pipe wall. Details of this boundary condition, applied to a channel flow case, are given by Kawamura et al. (1998). The computation was started with random initial conditions and run until a stationary state was achieved. The stationary state was determined by the total kinetic energy and scalar variance remaining approximately constant. The grid resolution and domain sizes (table 1) were chosen using previous DNS work of Kawamura et al. (1998).

Statistics were computed by averaging an instantaneous three-dimensional realization over the homogeneous (axial and azimuthal) directions. Ensemble averaging was then performed over several realizations that were separated by a time greater than the estimated integral time scale. For the SP the integral time scale was estimated using the centerline velocity and pipe diameter.

Reynolds number	2650 ($Re_\tau \approx 180$)
Schmidt number	0.71 and 5.00
Computational volume (x, y, z)	$2\pi R \times R \times 2\pi$
Grid number	$256 \times 128 \times 384$
Grid spacing (wall units)	$\Delta x^+ = 4.42$
	$\Delta y^+ = 0.178, 2.46$
	$R\Delta z^+ = 2.95$
Number of 3D samples	42
Time between samples	5t

Table 1: Straight pipe – computational conditions

Rotating Cylinder Simulation Details

The Reynolds number for the RC simulation was chosen on the basis of matching previous experimental work (Kataoka et al., 1977), and approximately matching wall shear stress to the SP simulation (indicated by Re_τ). Schmidt numbers were chosen to match the SP, table 2.

The boundary conditions were periodic in the axial and azimuthal directions and no slip at the inner and outer cylinder walls. Tangential velocity was set to a constant magnitude at the inner cylinder, and zero at the outer cylinder. For mass transfer the boundary conditions were periodic in the axial and azimuthal directions, and fixed concentration at the inner and outer cylinders. The inner cylinder concentration was given a finite magnitude while the outer cylinder concentration was set to zero.

Reynolds number	3200 ($Re_\tau = 200$)
Schmidt number	0.71 and 5.00
Radius ratio	$\eta = 0.617$
Axial wavelength	$\lambda = 2.29(R_2-R_1)$
Computational volume (x, y, z)	$2\lambda \times (R_2-R_1) \times 2\pi$
Grid number	256×128×384
Grid spaing (wall units)	$\Delta x^+ = 3.66$
	$\Delta y^+ = 0.35, 2.97$
	$R_1\Delta z^+ = 4.98$
Number of 3D samples	42
Time between samples	10t

Table 2: Rotating cylinder – computational conditions

The axial domain length of the simulation was chosen to accommodate two pairs of TV, where the size of the vortices was determined from experimental results (Kataoka et al., 1977). The grid resolution, table 2, was determined by matching the resolution in wall units to previous DNS of channel or pipe flow. The adequacy of

the domain size and grid resolution was investigated and found to be sufficient (Bilson, to be published).

Statistics were computed in the same manner as the SP. The integral time scale for the RC was estimated using the inner cylinder velocity and circumference at the outer cylinder.

RESULTS

Straight Pipe

The mean velocity and scalar, figure 2, show good agreement compared to the channel flow DNS of Kawamura et al. (1998). There is some over-prediction towards the pipe center for the present simulation, however this is a common difference observed between pipe and channel flow at low Reynolds numbers (Eggels et al., 1994). Fluctuating velocity shows very good agreement with Kawamura et al. (1998), figure 3. The scalar also displays very good agreement with Kawamura near the wall, but for regions away from the wall the present simulation over-predicts the scalar fluctuation. Scalar flux is shown in figures 4 and 5 for Sc=0.71 and Sc=5.0. Agreement is very good near the wall, however for $y^+ \geq 15$ the present results tend to overpredict Kawamura's results. Another difference is the waviness of the total scalar flux, especially at Sc=5.0.

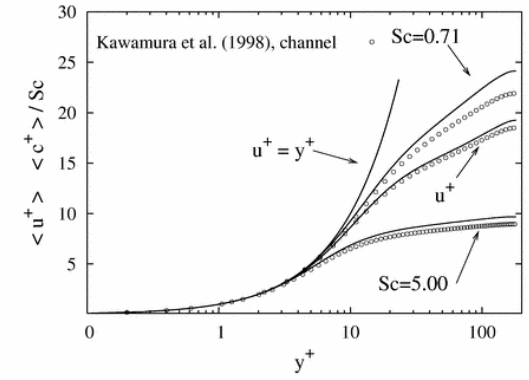

Figure 2: Straight pipe - mean velocity and scalar for Sc=0.71 and Sc=5.0

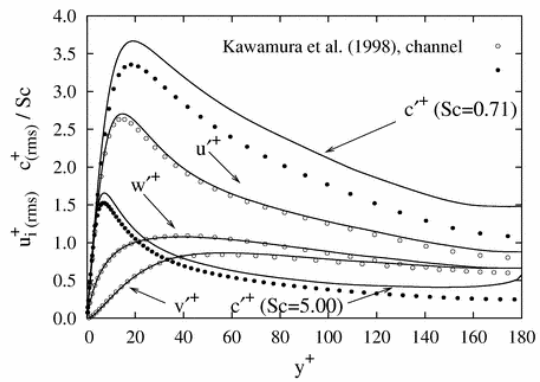

Figure 3: Straight pipe - fluctuating velocity and scalar for Sc=0.71 and Sc=5.0

Generally the DNS code was working well. The differences between the present results and those of Kawamura were been caused by the boundary condition used to drive the flow influencing the convergence of statistics. Kawamura used a constant pressure drop, which is the same as constant wall shear stress. The present simulations were run with constant pressure drop and better convergence of statistics was achieved with the same number of samples (Bilson, to be published).

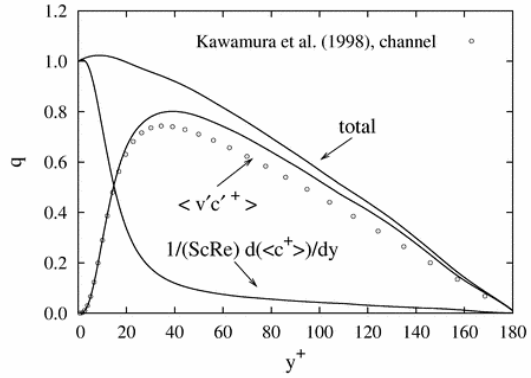

Figure 4: Straight pipe – turbulent and molecular scalar flux for Sc=0.71

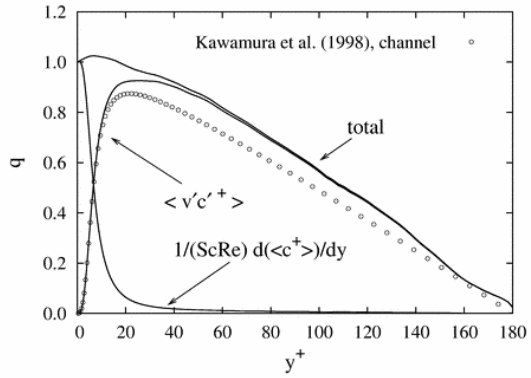

Figure 5: Straight pipe – turbulent and molecular scalar flux for Sc=5.0

Rotating Cylinder

The interpretation of results for the RC requires more detailed analysis than the SP because of the TV motion. Several averages, velocity fluctuations, and conventions are defined in table 3. Because the TV motion is two-dimensional the results should be presented to reflect this. However in this paper results are averaged in the axial direction for easier presentation. Results will be reported for the inner cylinder only.

The Sherwood number at the outer cylinder was compared to experiments (Kataoka et al., 1977) with very good agreement observed, figure 6. Variation from experiment was due to the higher Schmidt number of the experiments (Sc≈3000). Note that the Sc=5.0 case showed better agreement with the experiments than the Sc=0.71 case. Two pairs of vortices were formed for the RC simulation, figure 7. A secondary vortex pair was also identified at the locations $2x/\lambda = 1.0$ and $2x/\lambda = 3.0$. This was responsible for the kink in the Sherwood number profile.

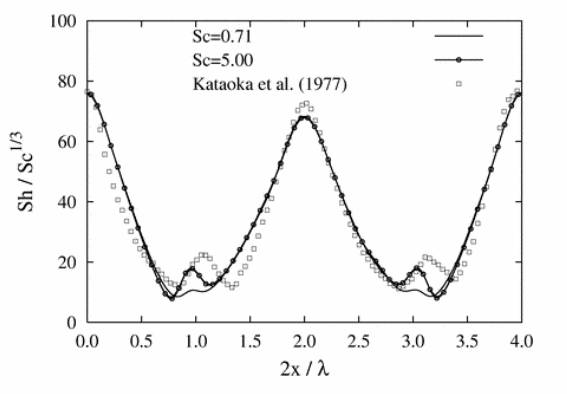

Figure 6: Rotating cylinder – Sherwood number at the outer cylinder

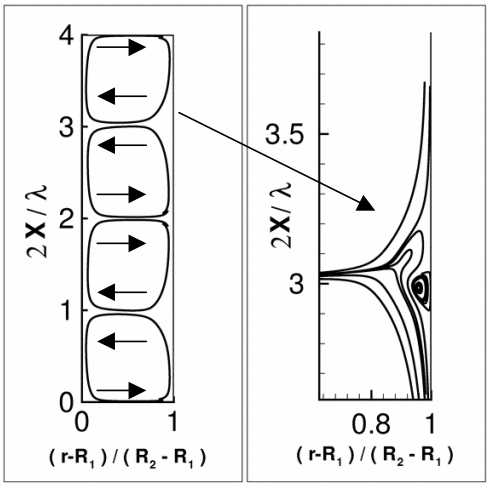

Figure 7: Rotating cylinder – Taylor vortex visualization

The total Sherwood number was computed at the inner cylinder (based on the concentration difference between the cylinders). For Sc=0.71 it was 20.07, and for Sc=5.0 it was 40.69. In the SP the Sherwood number (based on difference between wall concentration and bulk concentration) was 20.4 for Sc=0.71 and 42.69 for Sc=5.0. The agreement in overall scalar transfer rates confirms that shear stress matching will give similar overall scalar transport rates for the cases being considered here.

For the SP a linear profile was observed for the mean velocity field up to $y^+ \approx 5$, $y^+ \approx 6$ for the mean scalar field at Sc=0.71, and $y^+ \approx 3.5$ for Sc=5.0, figure 2. For the RC the velocity and scalar profiles are still linear near the wall, figure 8, however the deviation from linearity starts nearer to the wall (e.g. at the inner cylinder $y^+ \approx 2$ for the velocity field, $y^+ \approx 3$ for Sc=0.71, and $y^+ < 2$ for Sc=5.0). This indicates that the viscous and diffusion sub-layers are not as thick in the RC.

The fluctuating velocity shows a remarkable similarity to the SP when the fluctuations due to the TV are removed, figure 9. However, the magnitude of the peak fluctuations is much less than the SP. When the fluctuations due to TV are retained the behavior is very different to the SP, yet the peak magnitudes of the fluctuations are comparable. This indicates that the underlying turbulent velocity fluctuations might be similar in both configurations.

u	instantaneous variable
$< u >_{xzt}$	one dimensional mean
$u' = u - < u >_{xzt}$	fluctuation due to turbulence and TV
$< u >_{zt}$	two dimensional mean
$u'' = u - < u >_{zt}$	fluctuation due to turbulence
$u' - u''$	fluctuation due to TV
$<\bullet>$	implies $<\bullet>_{xzt}$ unless otherwise stated

Table 3: Averages and fluctuations for the RC – subscripts denote coordinate over which averaging has been performed

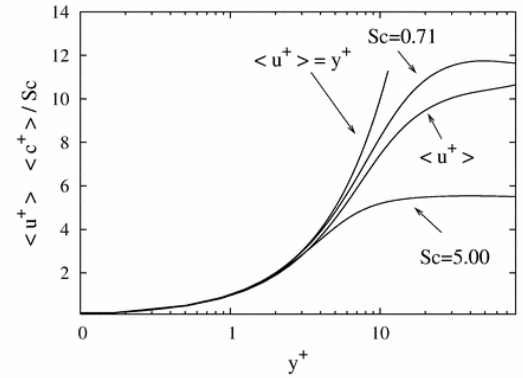

Figure 8: Rotating cylinder – mean velocity and scalar for Sc=0.71 and Sc=5.0 at the inner cylinder in wall units

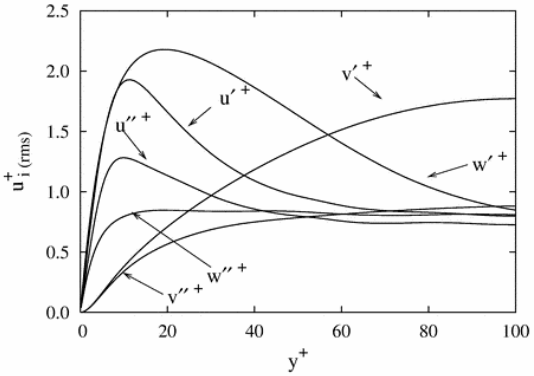

Figure 9: Rotating cylinder – velocity fluctuations at the inner cylinder in wall units

In the RC the scalar fluctuation due to turbulence and TV motion, figure 10, when compared with the streamwise velocity fluctuation shows a similar behavior to the SP (i.e. similar curve shapes). When the contribution of the TV motion is removed the streamwise velocity fluctuation and scalar fluctuation profiles start to show different profile shapes and it may indicate that turbulent transport mechanisms in the SP and RC are different.

The scalar flux due to molecular diffusion and turbulent and/or TV motion is shown in figure 11. There is a large scalar flux due to the TV motion, and only small molecular and turbulent components. Such a large convection transport mechanism does not occur in the SP. At higher Schmidt numbers there is a larger contribution from the turbulent transport near the wall, and the influence of convection reaches closer toward the cylinder walls. For regions very close to the cylinder walls the dominant transport mechanism is molecular diffusion, which is equivalent to the SP.

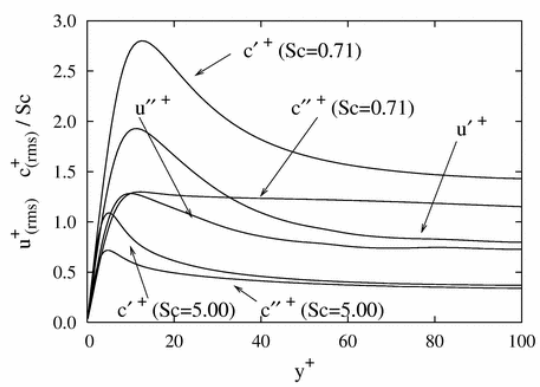

Figure 10: Rotating cylinder – axial velocity and scalar fluctuations (Sc=0.71 and Sc=5.0) at the inner cylinder in wall units

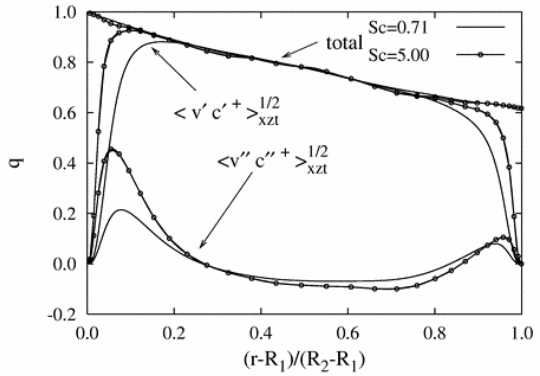

Figure 11: Rotating cylinder – scalar flux at Sc=0.71 and Sc=5.00

CONCLUSION

The overall scalar transport rate is virtually identical in the two configurations with matched mean wall shear stress. However, the results show that scalar transport mechanisms in the RC are quite different to the SP, if the results are interpreted in a two-dimensional sense (i.e. separated into contributions from the mean, TV motion and turbulence motion). The TV motion makes up a significant fraction of the overall scalar transport. The consequence of this may be significant for RC experiments and subsequent transfer to the SP. If measurements in the RC were made at a few selected axial points on the cylinder the results would reflect a two-dimensional interpretation. Significant errors could occur when attempting to compare to SP results based on fully developed turbulence.

Acknowledgements

The computer resources for the simulations reported were provided by the Australian Partnership for Advanced Computing (APAC), and the Queensland Parallel Supercomputing Foundation (QPSF).

REFERENCES

AKSELVOLL, K. *Large eddy simulation of turbulent confined jets and turbulent flow over a backward facing step*, Ph.D. Thesis, Department of Mechanical Engineering, Stanford University, 1995.

AKSELVOLL, K. and MOIN, P., (1996), "An efficient method for temporal integration of the Navier-Stokes equations in confined axisymmetric geometries", *Journal of Computational Physics*, **125,** 454-463.

ANDERECK, C.D., LIU, S.S., and SWINNEY, H.L., (1986), "Flow regimes in a circular Couette system with independently rotating cylinders", *Journal of Fluid Mechanics*, **164,** 155-183.

BILSON, M.J. *Turbulent Flow and Mass Transport in the Rotating Cylidner*, Ph.D. Thesis, Division of Mechanical Engineering, The University of Queensland, to be published.

COLES, D., (1965), "Transition in circular Couette flow", *Journal of Fluid Mechanics*, **21,** 385-425.

EGGELS, J.G.M., UNGER, F., WEISS, M.H., WESTERWEEL, J., ADRIAN, R.J., FRIEDRICH, R., and NIEUWSTADT, F.T.M., (1994), "Fully developed turbulent pipe flow: a comparison between direct numerical simulation and experiment", *Journal of Fluid Mechanics*, **268,** 175-209.

EISENBERG, M., TOBIAS, C.W., and WILKE, C.R., (1954), "Ionic mass transfer and concentration polarization at rotating electrodes", *Journal of the Electrochemical Society*, **101,** 306-319.

GABE, D.R., WILCOX, G.D., GONZALES-GARCIA, and WALSH, F.C., (1998), "The rotating cylindrical electrode: its continued development and application", *Journal of Applied Electrochemistry*, **28,** 759-780.

KATOAKA, K., DOI, H., and KOMAI, T., (1977), "Heat/mass transfer in Taylor vortex flow with constant axial flow rates", *International Journal of Heat and Mass Transfer*, **20,** 57-63.

KAWAMURA, H., OHSAKA, K., ABE, H., and YAMAMOTO, K., (1998), "DNS of turbulent heat transfer in channel flow with low to medium high Prandtl number fluid", *International Journal of Heat and Fluid Flow*, **19,** 482-491.

KOBAYASHI, M., MATSUBARA, K., and MAEKAWA, H., (1999), "Prediction of the turbulent Taylor vortex flow between concentric rotating cylinder", *International Journal of Transport Phenomena*, **1,** 245-254.

LIAO, C.B., JANE, S.J., and YOUNG, D.L., (1999), "Numerical simulation of three-dimensional Couette-Taylor flows", *International Journal for Numerical Methods in Fluids*, **29,** 827-847.

LEVICH, V.G., *Physicochemical Hydrodynamics.* Prentice-Hall, 1962.

POPE, S., *Turbulent Flows.* Cambridge University Press, 2000.

POULSON, B., (1983), "Electrochemical measurements in flowing solutions", *Corrosion Science*, **23,** 391-430.

POULSON, B., (1993), "Advances in understanding hydrodynamic effects on corrosion", *Corrosion Science*, **35,** 655-665.

SILVERMAN, D.C., (1984), "Rotating cylinder electrode for velocity sensitivity testing", *Corrosion*, **40,** 220-226.

SMITH, G.P., and TOWNSEND, A.A., (1982), "Turbulent Couette flow between concentric cylinders", *Journal of Fluid Mechanics*, **123,** 187-217.

YUU, S., and UMEKAGE, T., (1995), "Direct numerical simulation of the three-dimensional Navier-Stokes equations for turbulent circular Couette flows (Re=1500) and experimental verification", *Kagaku Kogaku Ronbunshu*, **21,** 886-895.